Molecular Biology of the Cell
Vol. 19, 4837–4851, November 2008

An α-Helical Extension of the ELMO1 Pleckstrin Homology Domain Mediates Direct Interaction to DOCK180 and Is Critical in Rac Signaling

David Komander,*†‡ Manishha Patel,§† Mélanie Laurin,§ Nadine Fradet,§ Ariane Pelletier,§ David Barford,* and Jean-François Côté§‖¶

*Section of Structural Biology, Chester Beatty Laboratories, Institute of Cancer Research, London SW3 6JB, United Kingdom; §Institut de Recherches Cliniques de Montréal, Montréal QC, Canada H2W 1R7; ‖Faculté de Médecine, Université de Montréal; Montréal, QC, Canada H3C 3J7; and ¶Division of Experimental Medicine, McGill University, Montréal, QC, Canada H3A 1A3

Submitted April 3, 2008; Revised August 15, 2008; Accepted August 22, 2008
Monitoring Editor: Josephine C. Adams

The mammalian DOCK180 protein belongs to an evolutionarily conserved protein family, which together with ELMO proteins, is essential for activation of Rac GTPase-dependent biological processes. Here, we have analyzed the DOCK180-ELMO1 interaction, and map direct interaction interfaces to the N-terminal 200 amino acids of DOCK180, and to the C-terminal 200 amino acids of ELMO1, comprising the ELMO1 PH domain. Structural and biochemical analysis of this PH domain reveals that it is incapable of phospholipid binding, but instead structurally resembles FERM domains. Moreover, the structure revealed an N-terminal amphiphatic α-helix, and point mutants of invariant hydrophobic residues in this helix disrupt ELMO1-DOCK180 complex formation. A secondary interaction between ELMO1 and DOCK180 is conferred by the DOCK180 SH3 domain and proline-rich motifs at the ELMO1 C-terminus. Mutation of both DOCK180-interaction sites on ELMO1 is required to disrupt the DOCK180-ELMO1 complex. Significantly, although this does not affect DOCK180 GEF activity toward Rac in vivo, Rac signaling is impaired, implying additional roles for ELMO in mediating intracellular Rac signaling.

INTRODUCTION

DOCK180 family members are conserved bona fide guanine nucleotide exchange factors (GEFs) for Rho GTPases (Cote and Vuori, 2007). A subgroup of these proteins, the CDM members (*Caenorhabditis elegans* Ced-5, *Drosophila* Myoblast City, and mammalian DOCK180), regulate several Rac-dependent biological processes including phagocytosis of apoptotic cells, cell migration, axon pathfinding, and myoblast fusion in vivo (Rushton *et al.*, 1995; Wu and Horvitz, 1998; Wu *et al.*, 2002; Li *et al.*, 2008). Mechanistically, DOCK proteins rely on a conserved DOCK homology region (DHR)-2 domain to promote the GDP/GTP exchange of Rho GTPases (Brugnera *et al.*, 2002; Cote and Vuori, 2002). DOCK proteins are also endowed with a conserved DHR-1 domain capable of direct interaction with phosphoinositides (PI), in particular phosphatidylinositol-(3,4,5)-trisphosphate (PtdIns(3,4,5)P_3; Cote *et al.*, 2005), and this activity appears to be important in Rac-mediated cell polarity and migration in addition to myoblast fusion (Cote and Vuori, 2007).

The identification of *C. elegans Ced-12* in a screen for genes that control necrotic and apoptotic cell phagocytosis (Chung *et al.*, 2000) led to the recognition of a unique family of highly conserved engulfment and motility (ELMO) family proteins in eukaryotes (Gumienny *et al.*, 2001; Wu *et al.*, 2001; Zhou *et al.*, 2001). ELMO proteins physically interact with a subset of DOCK180-related proteins (Meller *et al.*, 2005), including DOCK180 (DOCK1) and DOCK2–5, characterized by the presence of an amino-terminal Src homology (SH)-3 domain (Grimsley *et al.*, 2004; Hiramoto *et al.*, 2006). The remaining DOCK-related proteins, including DOCK6–8 and DOCK9–11/Zizimin1–3, lack a discernable SH3 domain and have not been reported to physically interact with ELMO proteins.

Several of the biological functions of DOCK180 characterized to date have been demonstrated to also require ELMO proteins. One established model proposes the idea of a bipartite exchange factor formed from DOCK180 and ELMO (Brugnera *et al.*, 2002), supported by the finding that coexpression of ELMO was required to stimulate the Rac GEF activity of DOCK180 (Brugnera *et al.*, 2002). However, in conflict with this model, we and others have found that DOCK180 displays substantial GEF activity when it is expressed alone in cells (Kiyokawa *et al.*, 1998; Cote and Vuori, 2002; Katoh and Negishi, 2003; Cote *et al.*, 2005; Hiramoto *et al.*, 2006). In support of this autonomous GEF model, the purified recombinant DHR-2 domain of DOCK180 is active

This article was published online ahead of print in *MBC in Press* (http://www.molbiolcell.org/cgi/doi/10.1091/mbc.E08–04–0345) on September 3, 2008.

† These authors contributed equally to this work.

‡ Present address: Division of Protein and Nucleic Acid Chemistry, MRC Laboratory of Molecular Biology, Hills Road, Cambridge CB2 0QH, UK.

Address correspondence to: Jean-François Côté (jean-francois.cote@ircm.qc.ca).

Abbreviations used: DHR-2, DOCK homology region 2; GEF, guanine nucleotide exchange factor; PH, pleckstrin homology; pro-rich, proline-rich.

toward Rac in vitro (Cote and Vuori, 2002). Nevertheless, it is generally agreed that ELMO is essential for physiological DOCK180 function, because interfering with the protein's properties, such as RhoG- or ERM-binding, results in impaired Rac-dependent cell migration and phagocytosis of apoptotic cells (Gumienny *et al.*, 2001; Wu *et al.*, 2001; Zhou *et al.*, 2001; Grimsley *et al.*, 2004; Bianco *et al.*, 2007).

The contribution of ELMO proteins for Rac signaling is poorly understood, and the mode of interaction between ELMO and DOCK proteins is not established. Some data indicate that the SH3 domain of DOCK180 binds to a proline-rich (pro-rich) motif at the C-terminus of ELMO (Gumienny *et al.*, 2001), and this interaction may regulate the activation state of DOCK180 (Lu *et al.*, 2005). However, because the ELMO/DOCK180 interaction is not completely blocked when either of these motifs are mutated (Lu *et al.*, 2005), additional contact regions between the two proteins presumably facilitates the high-affinity binding (Meller *et al.*, 2005).

A second interaction site between ELMO and DOCK180 was shown to involve, indirectly, the atypical PH-domain of ELMO (Lu *et al.*, 2004). In agreement with this, the ELMO PH domain was reported to provide a stabilizing effect toward a complex of nucleotide-free Rac and the DOCK180 DHR-2 domain (Lu *et al.*, 2004). It was found that in such a complex, the ELMO PH domain does not interact with DOCK180 directly, but rather stabilizes the critical reaction intermediate in *trans*, directly increasing the GEF activity of DOCK180 toward Rac by twofold (Lu *et al.*, 2004).

In this study we aimed to investigate the exact mechanism of interaction between ELMO1 and DOCK180 in order to assess the contribution of these two proteins in Rac GTP-loading and signaling. In contrast to a previous report (Lu *et al.*, 2004), we find that the atypical PH domain of ELMO1 directly interacts with DOCK180 in a Rac-independent and constitutive manner. Structural analysis of the atypical ELMO1 PH domain reveals an amphiphatic N-terminal α-helical extension, and we identify residues in this region required for DOCK180/ELMO1 interactions. Our data reveal that whereas the pro-rich region of ELMO1 and the SH3 domain of DOCK180 are dispensable for complex formation, these motifs are important for the physiological functions of ELMO1/DOCK180. Double mutation of both the ELMO1 amphiphatic helix and pro-rich motif is necessary to fully abrogate signaling from this complex. Importantly, we detect no difference in DOCK180 Rac GEF activity even in cells with defective ELMO1/DOCK180 signaling, arguing against a direct role of ELMO1 in DOCK180 GEF activity. Together, our findings provide novel insight into how ELMO proteins bind to and regulate DOCK proteins.

MATERIALS AND METHODS

Additional Material and Methods

Detailed information on the plasmids used in this study is available in the Supplementary Material (Supplementary Material and Methods).

Antibodies, Cell Culture, and Transfections

The following antibodies were obtained commercially: anti-DOCK180 (C-19 and H-4), anti-Myc (9E10), and anti-GFP (B-2) were from Santa Cruz Biotechnologies (Santa Cruz, CA), anti-Rac was from Millipore (Billerica, MA), and anti-FLAG M2 was from Sigma (St. Louis, MO). A polyclonal antibody was generated against DOCK180 using a His-tagged fragment of DOCK180 as an immunogen (His-DOCK180 422–619). HEK293T cells were cultured in DMEM supplemented with 10% fetal bovine serum, penicillin, and streptomycin (Invitrogen-BRL, Carlsbad, CA) and transfected by calcium phosphate or Lipofectamine 2000 (Invitrogen) using standard procedures. The Chinese hamster ovary (CHO) cell line, LR73 subclone, was maintained in α-MEM supplemented with 10% fetal bovine serum, penicillin, and streptomycin (Invitrogen-BRL) and transfected using Lipofectamine 2000 (Invitrogen) according to the manufacturer's instructions. Biochemical and cell biological studies were performed 24–48 h after transfection.

Immunoprecipitation, GST-Fusion Protein Pulldowns, and Rac-GTP Assays

Cells were lysed for 10 min in a buffer consisting of 50 mM Tris-HCl, pH 7.5, 150 mM NaCl, 1% NP-40, and 1× Complete protease inhibitor (Roche, Indianapolis, IN). For immunoprecipitation, clarified cell lysates were incubated with the appropriate antibody, and immune complexes were allowed to form for 1 h at 4°C. Protein A-Sepharose was added for 30 min to isolate the immune complex. For glutathione *S*-transferase (GST)-fusion protein pulldowns, the GST-fusion proteins were expressed in bacteria and purified on glutathione-Sepharose 4B according to manufacturer's instruction (Amersham, Piscataway, NJ). Equal amounts of the various GST-fusion proteins bound to glutathione Sepharose 4B were next incubated with cell extracts (500 μg of protein per condition). In both types of assays, the beads were washed three times with lysis buffer, and the bound proteins were analyzed by SDS-PAGE and immunoblotting. The GTP-loading status of Rac in CHO LR73 and HEK293T cells was analyzed by GST-PAK-PBD affinity precipitation as described previously (Cote and Vuori, 2002). Rac activation was quantified by densitometry analysis using ImageJ software (http://rsb.info.nih.gov/ij/). Signal for Rac-GTP was normalized to total Rac present in the cell lysate.

Cell Morphology and Cell Migration Assays

LR73 cells transfected with the indicated plasmids were subject to cell morphology or migration assays as previously described (Cote *et al.*, 2005). Briefly, cells were transfected with the indicated plasmids and serum-starved (0.5% FBS) overnight. Cells were gently detached (0.01% trypsin and 5 mM EDTA in Hanks' balanced solution), washed in fibroblast basal media (Cambrex, East Rutherford, NJ) supplemented with 0.5% BSA and 100,000 cells were then allowed to spread for 2 h before fixing with 4% paraformaldehyde. Cells were permeabilized with 0.2% Triton X-100 in PBS and blocked in PBS-1% BSA before staining with anti-DOCK180 (H4), DAPI (Invitrogen), and phalloidin (Invitrogen). The remainder of the cells was lysed to verify the expression levels of the exogenous proteins by Western blotting. For migration assays, the cells were transfected with pEGFP-C2 (0.5 μg, in addition to the indicated plasmids) as a tracker and were prepared as described above. Cells, 100 000, were loaded, in duplicate for each condition, in modified Boyden Chambers (Costar, Cambridge, MA) for which the underside of the membrane was precoated with 10 μg/ml fibronectin (BD Biosciences, San Jose, CA). Cells were allowed to migrate for 4 h before fixation in 4% paraformaldehyde. Cell in the upper chambers were mechanically removed using cotton swabs. Green fluorescent protein (GFP)-positive cells that migrated to the underside were counted from three to five independent fields on each membrane (20× magnification). The remainders of the cells were lysed to verify the expression levels of the exogenous proteins. For both assays, cells were photographed using a Leica DM4000 microscope (Deerfield, IL) equipped with a Retiga EXi (QImaging, Burnaby, BC, Canada) camera. ANOVA and all pairwise multiple comparison procedures (Holm-Sidak method) were performed for statistical analysis ($n = 6$ for each condition).

Lipid-binding Assays

GST ELMO1, ELMO1 532–707, BTK PH domain, and His DOCK180 DHR-1 were produced in bacteria and purified as previously described (Cote *et al.*, 2005). Purified proteins were quantified and 1 μg of each was used in lipid-coated beads pulldown (Echelon Biosciences, Salt Lake City, UT) exactly as previously described (Cote *et al.*, 2005).

In Vitro Transcription/Translation

The T7 TnT system (Promega, Madison, WI), and ^{35}S methionine was used, according to manufacturer's instruction, to generate the radiolabeled recombinant DOCK180 protein fragments. Interaction between DOCK180 and the ELMO1 GST-fusion proteins, performed as described above, were detected by Amplify-enhanced autoradiography (Applied Biosystems, Foster City, CA).

Protein Purification for Structural Studies

Three C-terminal human ELMO1 constructs (532–675, 532–707, 532–727), encompassing the PH domain, were cloned into the pGEX6-P1 vector, which contains a PreScission protease-cleavable GST tag. The fusion proteins were expressed in BL21-DE3 cells overnight at 25°C after induction with 150 μM IPTG at an OD_{600} of 0.8. Cells were lysed in buffer A (300 mM NaCl, 25 mM Tris, pH 8.50, 5 mM DTT, and 1 mM EDTA) complemented with 1 mg/ml lysozyme, 0.1 mg/ml DNAse I, and Complete protease inhibitor tablets (Roche), and sonicated at 4°C. Insoluble material was removed by centrifugation for 30 min at 40000 × *g*, and the lysate was incubated with glutathione Sepharose 4B resin (Amersham) for 1 h at 4°C. The resin was washed with 100 ml buffer A, 500 ml buffer A with 500 mM sodium chloride, and 200 ml buffer A with 200 mM sodium chloride. GST-PreScission protease was added (0.1 mg/ml), and the resin was incubated overnight at 4°C with agitation. The eluate, containing the ELMO1 PH domain, was collected, concentrated to 5

ml, and further purified on a Superdex75 gel filtration column, coupled to a 5-ml HiTrap glutathione Sepharose column (Amersham) to clear residual GST and GST-PreScission protease. The protein was concentrated in VivaSpin concentrators (VivaScience, Hannover, Germany; 10,000 MW cutoff) to a maximum concentration of 19 mg/ml, and dynamic light scattering indicated a monodisperse, nonaggregated sample. A 2-l bacterial culture produced up to 80 mg of pure ELMO1 PH for all constructs tested.

Crystallization

Crystallization screening was performed with all three ELMO1 PH proteins in a sitting drop setup by mixing 1 μl protein with 1 μl mother liquor. Although crystals were obtained from all constructs, diffracting crystals were only obtained for the shortest ELMO1 PH domain (532–675), from mother liquor containing 2.1 M sodium malonate, pH 6.75. Hexagonal crystals grew after 2 d, and reached a maximum size of $0.3 \times 0.3 \times 0.3$ μm after 7 d. The protein crystals were flash-frozen in a nitrogen cryo-stream without further cryo-protection. For experimental phasing, ELMO1 PH domain crystals were soaked in mother liquor enriched with 1 mM EMTS (ethyl mercury thiosalicylate) for 60 min, and back-soaked for 20 s in EMTS-free mother liquor before freezing.

Data Collection and Structure Determination

Data on ELMO1 PH crystals were collected at the European Synchrotron Radiation Facility (ESRF, Grenoble, France) station ID23–1. Native data were collected to 2.30-Å resolution, and derivative data with 22-fold anomalous multiplicity at the Hg edge (1.0086 Å) were collected to 3.0-Å resolution. The crystals displayed the high symmetry space group $P6_122$, which facilitated anomalous data collection (see Table 1 for data collection statistics). The data were processed with Mosflm and Scala from the CCP4 suite (Bailey, 1994). The structure was solved in a SIRAS experiment, using SHELX/hkl2map (Pape and Schneider, 2004), and SHARP (Bricogne *et al.*, 2003). SHARP determined a solvent content of 68%, with two molecules/AU and a Matthews coefficient of 4.8. Excellent phases were obtained, and automated model building with ArpWarp (Morris *et al.*, 2003) built ~85% of the model. Alternating further rounds of model building in Coot (Emsley and Cowtan, 2004) and refinement, initially with CNS-simulated annealing (Brunger *et al.*, 1998), and subsequently using TLS restrained refinement in Refmac5 (Vagin *et al.*, 2004), were performed, leading to the final refinement statistics in Table 1.

RESULTS

The Atypical PH Domain of ELMO1 Directly Interacts with DOCK180

We initiated a detailed study to analyze which ELMO region is involved in the interaction with DOCK180. ELMO proteins contain three main conserved regions (Figure 1A. The N-terminal region (residues 1–280, ELMO1 numbering) binds to RhoG (Katoh and Negishi, 2003; Hiramoto *et al.*, 2006), ERM proteins (Grimsley *et al.*, 2006; Handa *et al.*, 2007), and *Salmonella* IpgB1 (Handa *et al.*, 2007). The middle domain comprises an ELMO-domain (318–491), specific to ELMO proteins (Bowzard *et al.*, 2007). At the C-terminus, ELMO proteins contain an atypical PH domain (555–676; Zhou *et al.*, 2001). Lastly, a pro-rich motif (707–714) typical of SH3-interacting proteins and implicated in interactions with DOCK180 (Lu *et al.*, 2004), is located at the extreme C-terminus.

Secondary structure prediction of the C-terminal region of ELMO1 (residues 532–727) was performed (data not shown). In these analyses, α-helical regions were predicted both N-terminal (536–557) and C-terminal (679–697) to the annotated PH domain (Figure 1A, light blue regions). Using GST fusion proteins of the ELMO1 PH domain with and without the flanking regions, we tested the ability of these fragments to bind DOCK180. GST-tagged ELMO1 (532–707), containing both flanking regions, could robustly precipitate DOCK180 (Figure 1B). The flanking regions were crucial for the observed interaction, because deletion on the N-or C-terminal side (GST-ELMO1 555–707 and GST ELMO1–532-675, respectively) reduced DOCK180 binding significantly (Figure 1B). These results are in agreement with a previous report (Lu *et al.*, 2004), with the important difference that in that study, Rac1 was required to bridge the interaction between DOCK180 and ELMO1. We find a robust interaction between DOCK180 and ELMO1 in the absence of Rac1 both in vitro and in vivo.

Involvement of the DOCK180 SH3 Domain in ELMO1 Binding

DOCK180 contains an SH3 domain at its N-terminus, and ELMO1 contains a pro-rich motif (PxxP) at its C-terminus (Figure 1A). We analyzed the contribution of this potential interaction in the formation of the DOCK180/ELMO1 complex. As indicated in Figure 1B, ELMO1 (532–707), devoid of the pro-rich motif, robustly interacted with DOCK180, indicating that a SH3/PxxP interaction is dispensable for complex formation. Furthermore, GFP-fusion proteins of the ELMO1 PH domain, with or without the PxxP motif, were tested for their ability to coimmunoprecipitate with DOCK180. These experiments revealed that, in cells, the PH domain of ELMO1 (residues 532–707) is the minimal domain capable of binding to DOCK180 (Figure 1C). However, the addition of the pro-rich region of ELMO1 PH seemed to enhance its ability to interact with DOCK180 (Figure 1C).

To understand the contribution of the DOCK180 SH3 domain in the interaction with ELMO1, the proline residues 707, 710–712, 714, and 717 of ELMO1 were mutated to alanines ($ELMO1^{PxxP}$). Coimmunoprecipitation experiments of myc-tagged $ELMO1^{WT}$ and $ELMO1^{PxxP}$ in HEK293T cells indicated that both proteins interacted to an equivalent extent with exogenously expressed DOCK180 (Figure 1D). For the reverse experiment, DOCK180 lacking the SH3 domain ($DOCK180^{\Delta SH3}$) and a mutant in which a conserved Trp residue in the SH3 domain of DOCK180 was mutated to Lys ($DOCK180^{W45K}$), abolishing the binding of the SH3 domain to PxxP sequences (Tanaka *et al.*, 1995), were tested for their ability to bind $ELMO1^{WT}$ or $ELMO1^{PxxP}$. GST-tagged full-length $ELMO1^{WT}$ and $ELMO1^{PxxP}$ bound equally well to DOCK180, $DOCK180^{\Delta SH3}$, and $DOCK180^{W45K}$ in pulldown experiments (Figure 1E). These results indicate that the DOCK180/ELMO1 interaction is not dependent on the additional SH3/PxxP interaction, although in vivo, such an interaction might well exist. However, it is also possible that both motifs have additional functions and/or binding partners in cells that contribute to the cellular function of the DOCK180/ELMO complex (see below).

Structural Analysis of the ELMO1/DOCK180 Interaction

Our data indicated that on ELMO1, the PH domain and its flanking regions mediate the principle interactions responsible for complex formation with DOCK180. To understand the interaction between ELMO1 and DOCK180 in molecular detail, we initiated structural studies of the ELMO1 PH domain (Figure 2A). The ELMO1 PH domain is classified as a false-negative PH domain in ProSite (PS50003; Hulo *et al.*, 2008), as it does not fit the canonical PH domain profile, and therefore sequence comparison with crystallized PH domains is of limited value to aid domain boundary definition. Another crystallized member of this subgroup of PH domains is that of PDK1, which was found to form a unique N-terminal helical extension (Komander *et al.*, 2004). This prompted us to include the N-terminal flanking region of the ELMO1 PH domain in our constructs for crystallization. Three ELMO1 PH domain constructs were analyzed, comprising residues 532–675, 532–707, and 532–727. Diffraction quality protein crystals could only be obtained for the shortest construct, lacking the C-terminal flanking region (532–675). Diffraction data were collected to 2.3-Å resolution at the ESRF, and the structure was solved by SAD phasing using a mercury derivative. Excellent experimen-

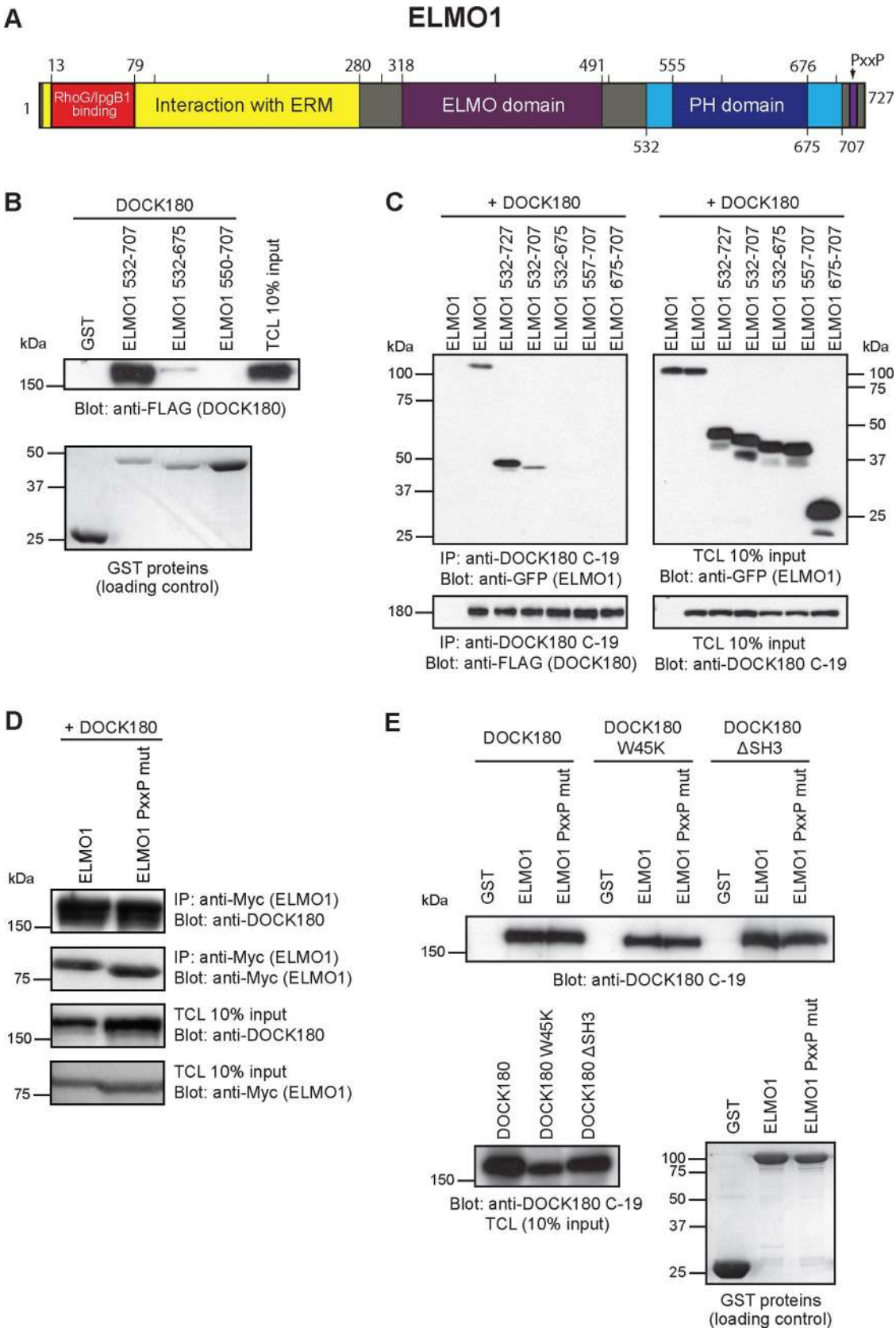

Figure 1. The atypical PH domain of ELMO1 directly interacts with DOCK180. (A) Domain architecture of ELMO1 (following ProSite annotation), indicating known protein interaction and functional regions. The N-terminal region of ELMO1 binds to RhoG (Katoh and Negishi, 2003), ERM proteins (Grimsley *et al.*, 2006), and *Shigella* IpgB1 (Handa *et al.*, 2007). The middle (ELMO) domain of ELMO1 has no assigned function, but is conserved in ELMO proteins. The C-terminal 200 amino acids encompassing the PH domain (blue) and flanking

Table 1. Data collection, phasing, and refinement statistics

	ELMO1 PH domain EMTS	ELMO1 PH domain native
Data collection		
Beamline	ID23–2	ID23–2
Wavelength (Å)	1.0086	1.0000
Space Group	$P6_122$	$P6_122$
Unit Cell (Å)	a,b = 165.47, c = 81.47	a,b = 166.02, c = 81.70
Resolution (Å)	80.0–3.00 (3.16–3.00)	40.0–2.30 (2.42–2.30)
Observed reflections	555933 (82449)	188356 (28101)
Unique reflections	13668 (1941)	29960 (4298)
Multiplicity	40.7 (42.5)	6.3 (6.5)
Completeness (%)	100.0 (100.0)	99.9 (100.0)
R_{merge}	0.124 (0.537)	0.058 (0.229)
$<I/\sigma I>$	35.5 (8.7)	22.7 (8.3)
Phasing statistics		
Anomalous completeness (%)	100.0 (100.0)	
Anomalous multiplicity	22.2 (22.5)	
FOM before/after DM	0.26/0.83	
Phasing power anomalous	1.96	
Phasing power isomorphous	1.55	
Refinement		
Reflections in test set		1504 (5%)
R_{cryst}		0.208
R_{free}		0.239
Number of groups		
Protein residues		288
Water		150
Wilson B (Å²)		43.1
<B>, protein (Å²)		19.1
<B>, water (Å²)		23.0
RMSD from ideal geometry		
Bond length (Å)		0.020
Bond angles (°)		1.9
Main chain bond (Å²)		1.3

Values in parentheses are for the highest resolution bin. All measured data were included in structure refinement.

tal phases were obtained and the structure was built and refined to a final R-factor of 0.208 (R_{free} = 0.239; Table 1). Two molecules of the ELMO1 PH domain are present per asymmetric unit, which superpose with an RMSD of 1.0 Å (>132 Cα atoms). In the subsequent analysis we will focus on one molecule only.

Figure 1 (cont). regions (light blue) and the pro-rich C-terminus (purple) is the focus of this study. (B and C) The PH domain of ELMO with N- and C-terminal flanking regions interacts with DOCK180 and the flanking regions are important in the interaction. (B) GST-tagged versions of the indicated fragments of ELMO1 PH region were used to pulldown FLAG-tagged DOCK180 from HEK293T lysate. (C) Similar experiment to B with GFP-tagged ELMO1 variants. HEK293T cells were cotransfected with the indicated plasmids, and lysates were subjected to immunoprecipitation with an anti-DOCK180 antibody. (D) The $ELMO1^{PxxP}$ mutant is not sufficient to abrogate DOCK180/ELMO binding in vivo. Lysates of HEK293T cells transfected with the indicated plasmids were immunoprecipitated with an antibody against the Myc-epitope of ELMO1. Immunoblot analysis using anti-DOCK180 rabbit polyclonal and anti-Myc antibodies established the coprecipitation of DOCK180 and ELMO proteins. (E) Disruption of a possible SH3: PxxP interaction between DOCK180 and ELMO1 is not sufficient to uncouple DOCK180/ELMO1 binding in vitro. Purified GST, GST-$ELMO1^{WT}$, or GST-$ELMO1^{PxxP}$ were used in pulldown experiments using lysates from HEK293T cells transfected with $DOCK180^{WT}$, $DOCK180^{W45K}$, or $DOCK180^{\Delta SH3}$. The bound proteins were detected by immunoblotting with an anti-DOCK180 antibody (C-19).

Structure and Evolutionarily Conserved Features of the ELMO1 PH Domain

The crystallized ELMO1 construct contains two main structural features. The N-terminal 23 residues form a single extended α-helix (αN, residues 532–554), which, without break leads into the β1-strand of a subsequent canonical PH domain fold (residues 555–675; Figure 2A). This fold is defined by a three-stranded and a four-stranded β-sheet forming a sandwich structure that is capped on one side by a C-terminal α-helix (αC; Lemmon and Ferguson, 2000; Figure 2A). The C-terminal helix of the ELMO1 PH domain interacts with invariant hydrophobic residues of the N-terminal helix (Leu553, Leu556), which stabilizes the striking 70° angle between helices (Figure 2, A and B). Notably, the extended N-terminal helix in the ELMO1 PH domain is a unique feature of ELMO proteins, bearing no resemblance to the extension seen in the PDK1 PH domain (Komander *et al.*, 2004), nor has it been observed in any other PH domain structurally characterized to date.

We performed sequence analysis of ELMO1 PH domains from different species and also compared the three mammalian ELMO isoforms for conserved features in their PH domain region (Figure 2B). The PH domain including the N-terminal helix extension is well conserved throughout species from *Drosophila melanogaster* to *Homo sapiens* and contains a large number of invariable residues. Strong sequence conservation within the three isoforms of human and mouse ELMO proteins suggests very similar structures

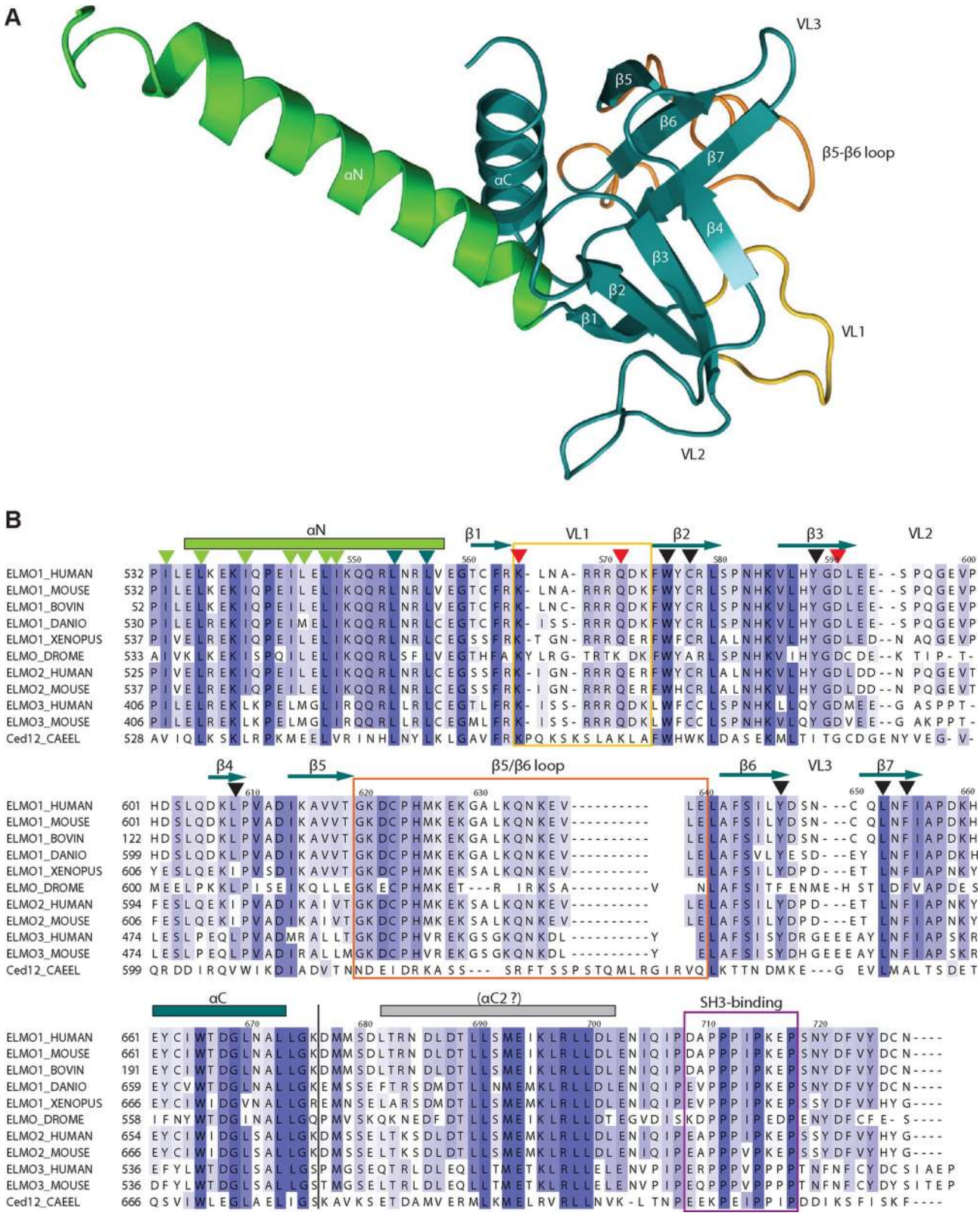

Figure 2. Structure of the ELMO PH domain and conservation in the ELMO family. (A) The structure of the ELMO1 PH domain (residues 532–675) is shown in cartoon representation. The αN helix is shown in green, the PH domain fold in teal, the VL1 region in yellow, and the β5/β6 loop is shown in orange. (B) A sequence alignment of the crystallized ELMO1 PH domain region and C-terminal residues from various species, as well as the ELMO2 and ELMO3 isoforms is shown. Secondary structure elements are indicated and labeled according to A, and a black line indicates the end of the crystallized construct. Boxes indicate the VL1 and β5-β6 loop regions highlighted in A. At the C-terminus, the SH3 binding region is boxed, and the predicted helical region (αC2), which is not part of the structure, is indicated. See supplementary text for additional information.

Table 2. DALI analysis of the ELMO1 PH domain fold

PH domain	PDB-ID	Z-score	RMSD (Å)	Aligned residues
PLCδ-IP3	1mai	10.5	2.4	96
DAPP1-IP4	1fao	9.0	2.5	86
Moesin	1ef1	8.8	2.3	83

of the PH domain regions of ELMO proteins (Figure 2B). The sequence similarity, length and conservation of loop insertions (V_L), and the large number of invariant residues indicates that the ELMO PH domain fold is conserved in all ELMO isoforms, indicating a general functional equivalence of this region in ELMO proteins.

The ELMO1 PH Domain Is Unable to Bind Phosphoinositides

To identify similar structures in the protein data bank, we performed a DALI search (Holm and Sander, 1993) with the PH domain region of ELMO1 (residues 554–675; Table 2). The highest similarity to the ELMO PH domain was found with the PH domain of phospholipase C δ (PLCδ) in complex with inositol (1,4,5)-trisphosphate (Ins(1,4,5)P_3; pdb-id 1mai, Z-score 10.5; Ferguson *et al.,* 1995; Figure 3B, Table 2), and with the PH domain of Dual Adaptor of Phosphotyrosine and 3-Phosphoinositides (DAPP1) in complex with inositol (1,3,4,5)-tetrakisphosphate (Ins(1,3,4,5)P_4; pdb-id 1fao, Z-score 9.0; Ferguson *et al.,* 2000; Figure 3C, Table 2). DAPP1 and PLCδ both contain insertions in the β5/β6 loop similar to ELMO1, probably accounting for the high Z-scores. Notably, DALI analysis did not detect similarities of the ELMO1 PH domain with PH domains from the other large family of Rho family GEFs that contain a catalytic Dbl-Homology (DH)/PH domain tandem.

The overall structural similarity of ELMO1 with PLCδ and DAPP1 suggested that the phospholipid-binding properties might be conserved and that the ELMO1 PH domain might have a role in localizing the ELMO1/DOCK180 complex to membranes. The common site of interaction with PIs in PH domains is created by three variable loops, connecting β1/β2 (VL1), β3/β4 (VL2), and β6/β7 (VL3), respectively, located opposite of the α-helices at the open side of the β-sheet sandwich (Ferguson *et al.,* 2000). The variable loops create a positively charged pocket for interaction with the negatively charged PIs (Figure 3). Two key basic residues are conserved in this pocket of PI-binding PH domains (Ferguson et al., 2000), namely a Lys residue on β1 located in the back of the pocket, which interacts with the D4-phosphates of Ins(1,4,5)P_3 or Ins(1,3,4,5)P_4, and an Arg residue in the β2-strand, which interacts with the adjacent phosphate group of the ligand (Figure 3B and C). In ELMO1, the Lys residue is conserved (Lys564); however, the Arg-equivalent residue is substituted by a Trp (Trp575), forming a hydrophobic rather than a positively charged base of the pocket (Figure 3A). More strikingly, the position of the guanidine group of the conserved Arg residue is structurally replaced by the side-chain carboxy-group of Asp590, which neutralizes the charge of Lys564, and in addition would repel a phosphate group of a bound PI-ligand (Figure 3A). Notably, residues Lys564, Trp575, and Asp590 are invariant in all ELMO PH domains (Figure 2B). Hence, ELMO PH domains display structural features incompatible with PI-binding analogously to PLCδ or DAPP1 (Figure 3, further analysis in Supplementary Material). In agreement with the structural results, we found that neither full-length ELMO1 nor the isolated ELMO1 PH domain were capable of specific binding to any phosphorylated PI in vitro, in lipid-coated beads pulldown experiments or phospholipid overlay assays (Supplementary Figure S1 and data not shown). We conclude that ELMO1 does not serve as a phospholipid-targeting module in the ELMO1/DOCK180 complex.

Further analysis of the ELMO1 PH domain fold revealed significant similarity with the F3 subdomain of FERM (Band 4.1, Ezrin, Radixin, Moesin) domains (see Figure 3D, Supplementary Material, and Supplementary Figure S2). Interestingly, in the context of FERM domains, the PI-binding site equivalent region is utilized as a protein–protein interaction site (Pearson *et al.,* 2000). Future work will address whether the similarly shaped ELMO PH domain interacts with protein motifs through this site.

Analysis of the N-Terminal Helical Extension of the ELMO1 PH Domain

The N-terminal helical extension is a defining feature of the ELMO1 PH domain, and this region is involved in several crystal lattice contacts, forming a tight dimer interaction with the second molecule in the asymmetric unit, and with a crystallographically related second dimer in the crystal lattice (Figure 4A, Supplementary Material and Supplementary Figure S3). These prominent helix–helix interactions suggest that the N-terminal α-helix might be involved in protein–protein interactions.

Further analysis shows that the N-terminal α-helix is amphiphatic in nature: hydrophobic Leu and Ile residues (Ile533, Leu536, Ile540, Ile544, Leu545, Leu547, and Ile548) are all located to one side of the helix, whereas the opposite surface shows a hydrophilic character (Figure 4, A and B). This pattern of Leu/Ile residues with a spacing of four amino acids is reminiscent of coiled-coil proteins, which often interact in a well-described coiled-coil or Leu-zipper manner. Examination of the electrostatic potential and conservation of this region indeed reveals a hydrophobic ridge spanning the entire length (27 Å) of the protruding helix (Figure 4B). Importantly, the involved Leu and Ile residues are fully conserved in ELMO proteins and Ced-12 (Figure 4C), indicating potential functional relevance.

The Hydrophobic Side of the ELMO1 αN Helix is a DOCK180-binding Surface

We tested whether the strikingly conserved hydrophobic residues of the αN helix were involved in DOCK180 binding. Fully conserved hydrophobic residues in ELMO1 were mutated to negatively charged residues (L536D, I544D, L545E, L547E, and I548D, hereafter termed ELMO$^{\alpha N}$) and the resulting Myc-tagged or GST fusion proteins expressed at similar levels with the wild-type proteins. The mutant proteins were tested for their ability to coimmunoprecipitate DOCK180. Although full-length ELMO1^{WT} and ELMO1^{PxxP} bound to DOCK180 (Figure 4D), ELMO1$^{\alpha N}$ and the ELMO$^{\alpha N/PxxP}$ double mutant completely lost their ability to interact with DOCK180 (Figure 4D). The same ELMO1 mutants (ELMO$^{\alpha N}$, ELMO1^{PxxP}, and ELMO$^{\alpha N/PxxP}$) expressed as GST proteins were also tested for their ability to precipitate with DOCK180 from cell lysates. In agreement with the above data, the ELMO1^{WT} and ELMO1^{PxxP} bound equally well to DOCK180 in pulldown experiments (Figure 4E). However, minimal but reproducible binding to DOCK180 could be observed for the ELMO1$^{\alpha N}$, whereas the double mutant ELMO1$^{\alpha N/PxxP}$ completely lost the ability to interact with DOCK180 (Figure 4E). To confirm these results, we also gen-

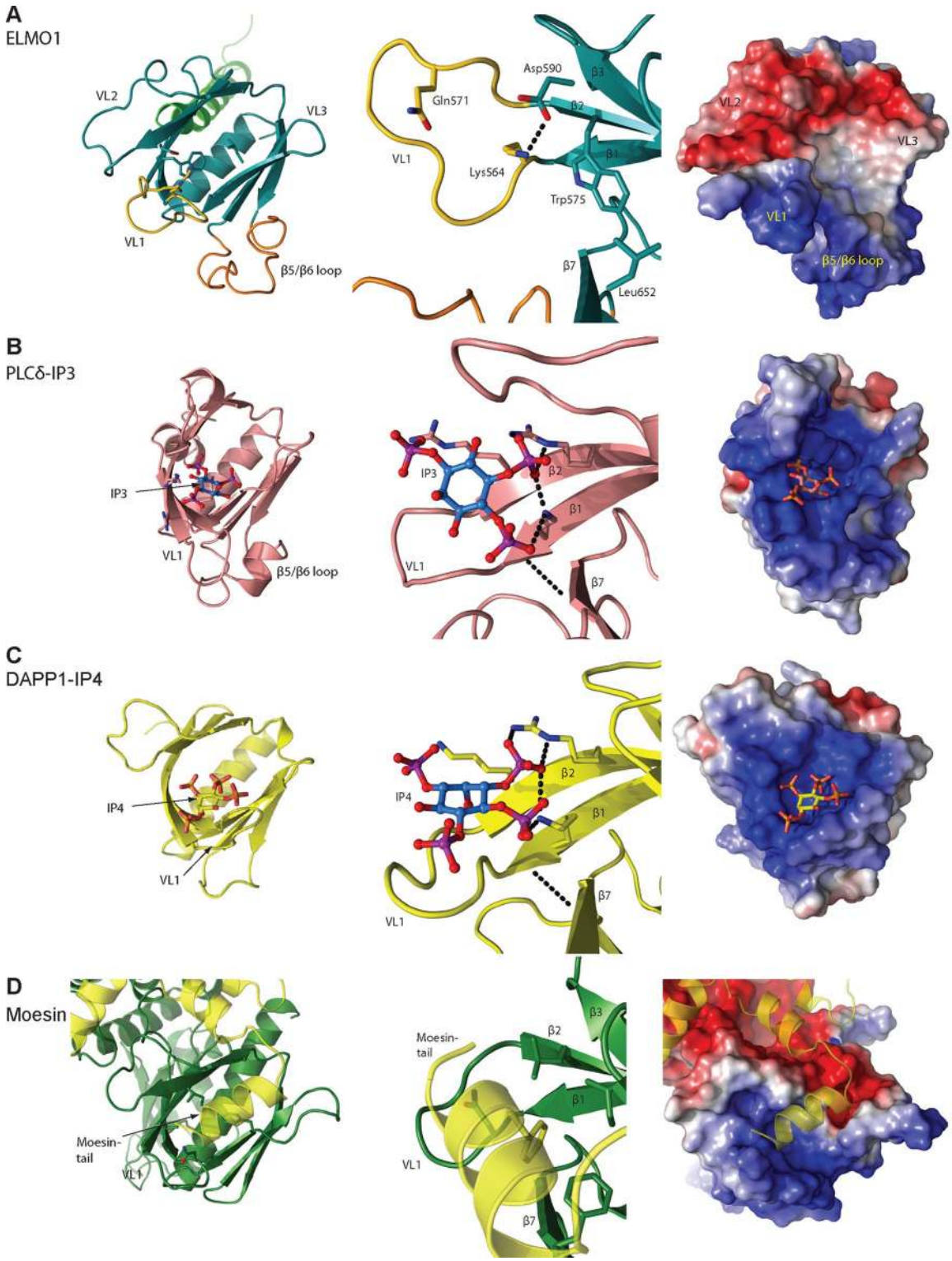

Figure 3. Comparison of the PH domain fold of ELMO with other PH domains. (A) Representation of the ELMO1 PH domain structure. Left, the PH domain fold is shown with an orientation looking into the putative ligand binding site; middle, the β1- and β2-strands and VL1 region is shown in cartoon representation, and key residues involved in PI-binding and ligands are drawn. Hydrogen bonds are indicated as black dotted lines. Right, an electrostatic surface potential calculated with APBS of the same view as to that on the left. Blue regions, positive surface potential; red regions, negative surface potential; white regions, uncharged. Key residues, loop regions, and ligands are labeled. (B) PLCδ PH domain in complex with Ins(1,4,5)P_3 (1mai; Ferguson *et al.,* 1995), shown as in A. The ligand is shown in stick representation with red oxygen and purple phosphorous atoms. (C) DAPP1 PH domain in complex with Ins(1,3,4,5)P_4 (1fao; Ferguson *et al.,* 2000). (D) F3 subdomain of Moesin bound to its C-terminal tail peptide in yellow (1ef1; Pearson *et al.,* 2000).

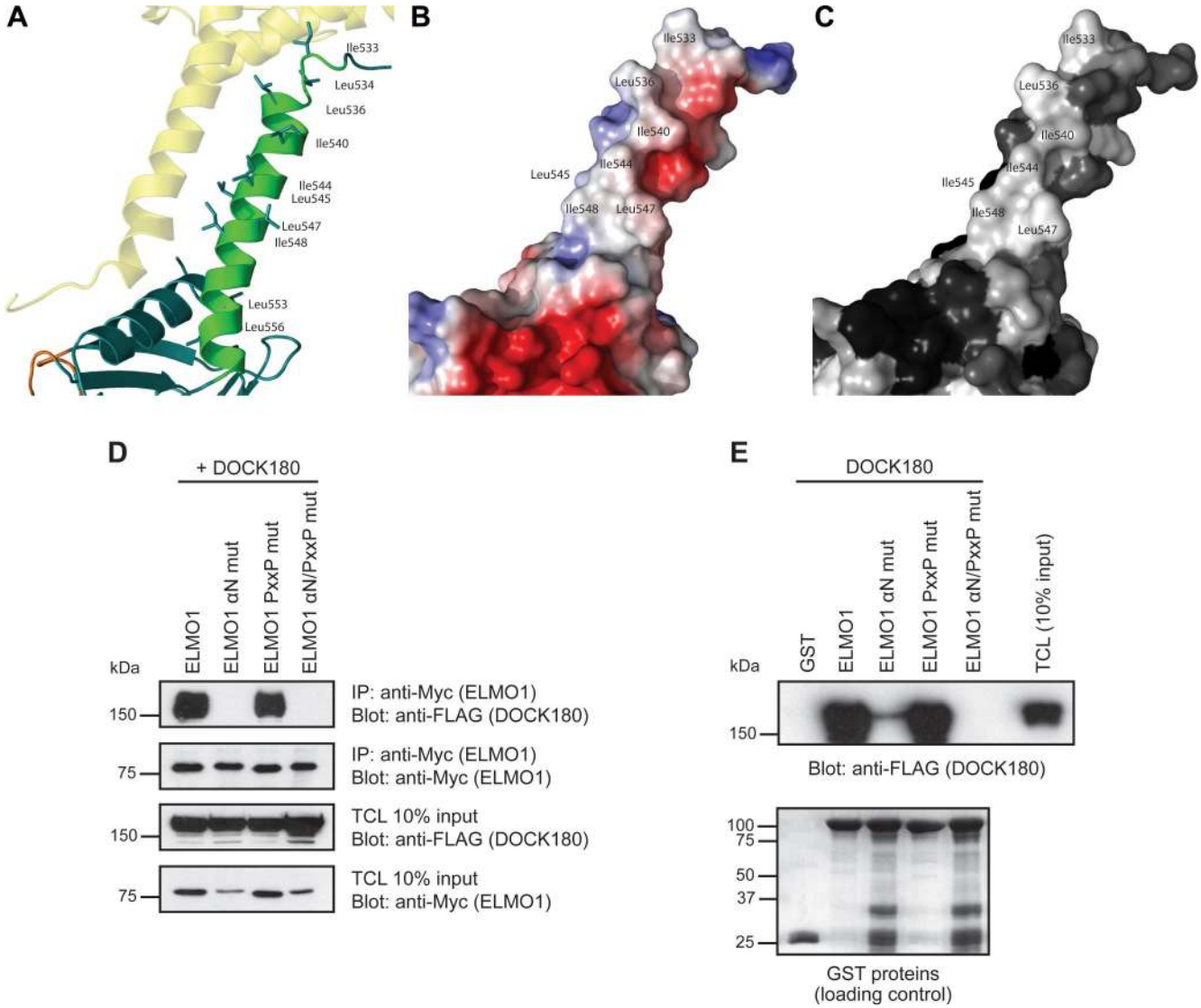

Figure 4. The extended N-terminal α-helix of ELMO1 PH domains is a DOCK180-binding site. (A) Cartoon representation of the N-terminal α-helix colored according to Figure 2A. Hydrophobic Leu and Ile residues are shown and labeled (see Figure 2B). The second molecule of the asymmetric unit is shown in yellow, interacting through the helix in an antiparallel manner but not employing the hydrophobic Leu/Ile residues; the Leu/Ile side chains of both molecules point toward the same side, generating a large hydrophobic platform that interacts with the same α-helical region of a crystallographically related dimer (also see Supplementary Figure S3). (B) Electrostatic surface potential calculated with APBS. Blue regions, positive surface potential; red regions, negative surface potential; white regions, hydrophobic. (C) The surface of the ELMO1 PH domain is colored from white (fully conserved) to black (no conservation). (D–E) Mutation of conserved hydrophobic residues in the αN-helix of the ELMO1 PH domain abolishes the DOCK180/ELMO1 interaction. (D) Lysates of HEK293T cells transfected with the indicated plasmids were immunoprecipitated with an antibody against the Myc-epitope (ELMO1). The coprecipitation of the various ELMO1 proteins and DOCK180 was analyzed via immunoblotting with anti-Myc (ELMO) and anti-FLAG (DOCK180) antibodies, respectively. (E) Lysates of HEK293T cells transfected with FLAG-DOCK180 were subjected to pulldown assays with GST-ELMO1 proteins. The precipitation of DOCK180 by the various ELMO1 fusion proteins was detected via immunoblotting with anti-FLAG (DOCK180).

erated similar mutants of ELMO1 with minimal mutations in the αN helix (ELMO1$^{L547E/I548D}$ and ELMO1$^{L547E/I548D/PxxP}$) and obtained identical results with respect to DOCK180 binding (Supplementary Figure S4). In addition, we also created an ELMO1 mutant in which the hydrophobic residues were mutated to alanine (ELMO1$^{L547A/I548A}$), instead of charged residues, and we demonstrated that this mutant lacks DOCK180-binding activity (Supplementary Figure S4). We conclude that we have identified a single helix on ELMO proteins, preceding the PH domain, which mediates direct hydrophobic interactions with DOCK180.

Identification of ELMO1-binding Sites on DOCK180

Having identified crucial regions within ELMO1 for DOCK180 binding, we attempted to map the reciprocal interaction sites on DOCK180. DOCK180 contains three annotated domains: an N-terminal SH3 domain and DHR-1 and DHR-2 domains that function as PI-binding and GDP/GTP exchange domains, respectively (Cote and Vuori, 2002; Cote *et al.*, 2005; Figure 5A). At its C-terminus, several pro-rich regions implicated in interactions with SH3 domains are found (Cote and Vuori, 2007). As mentioned above and in agreement with a previous study (Grimsley *et al.*, 2004), we

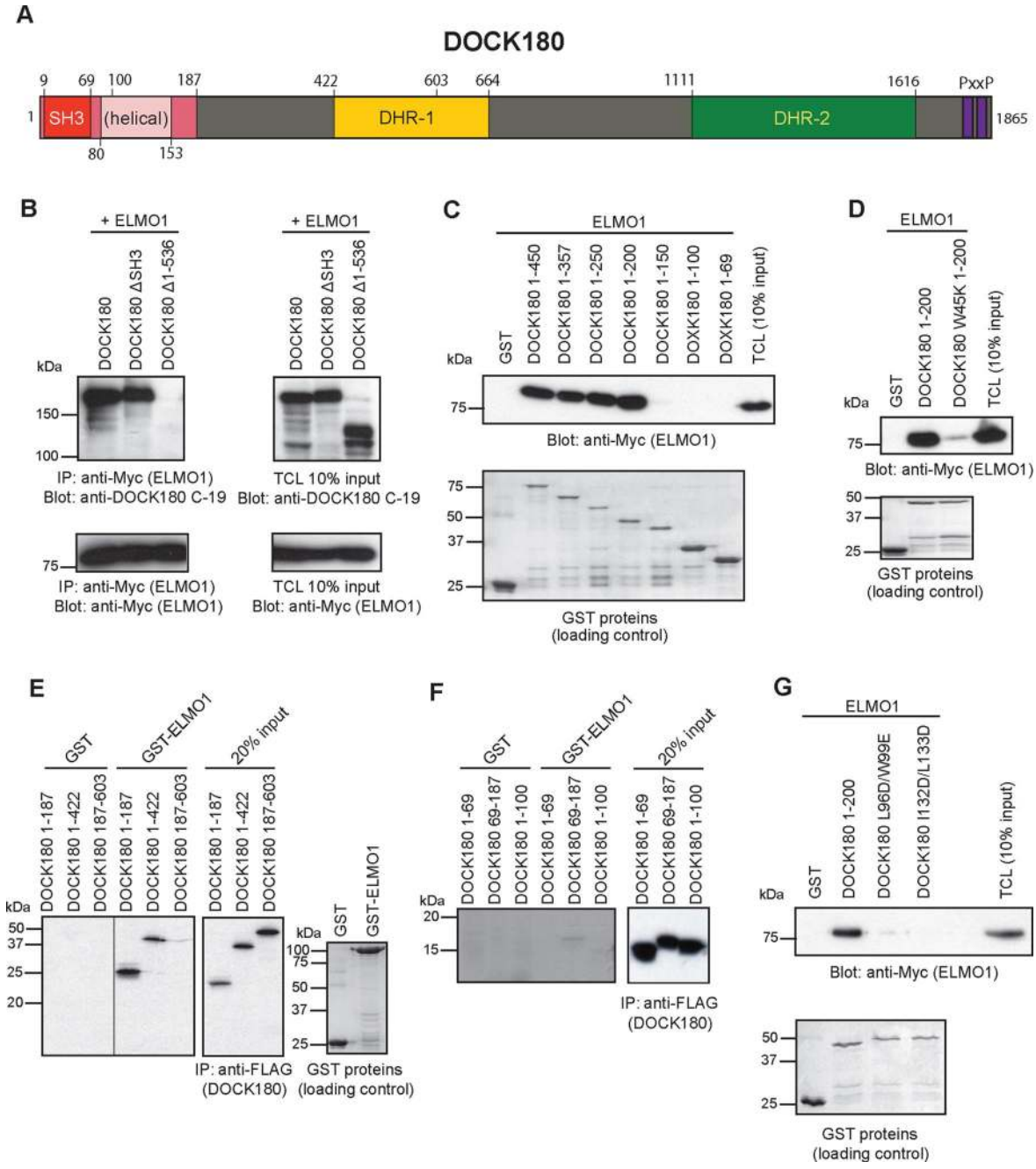

Figure 5. Identification of a novel ELMO1-binding region on DOCK180. (A) Schematic representation of DOCK180. The SH3 domain (red), DHR-1 (yellow), and DHR-2 (green) domains mediate protein interaction, PI binding, and Rac GDP/GTP exchange, respectively (Cote and Vuori, 2002; Cote *et al.*, 2005). Pro-rich motifs at the C-terminus (purple) bind in *trans* to SH3 domains (Cote and Vuori, 2007). The N-terminal 200 amino acids encompass the ELMO-binding region (Cote and Vuori, 2007; pink). (B) The N-terminal region of DOCK180 is essential for ELMO binding. HEK293T cells were transfected with $DOCK180^{WT}$, $DOCK180^{\Delta SH3}$, or $DOCK180^{\Delta 1-536}$, and cell lysates were subjected to immunoprecipitation against Myc-tagged ELMO1. Bound proteins were analyzed by immunoblotting using anti-DOCK180 and anti-Myc antibodies. (C) The first 200 amino acids of DOCK180 harbor the ELMO-binding domain. A panel of N-terminal GST-DOCK180 constructs was used in a pulldown assay with a lysate from Myc-ELMO1-transfected HEK293T cells. Bound proteins were detected by immunoblotting with an anti-Myc antibody. (D) The SH3 domain of DOCK180 contributes in ELMO1 binding. GST-fusion proteins of the residues 1–200 of $DOCK180^{WT}$ or $DOCK180^{W45K}$ were used in a pulldown assay with a lysate of Myc-ELMO1-transfected HEK293T cells. Bound proteins were detected by immunoblotting with an anti-Myc antibody. (E and F) Residues 69–187 of DOCK180 are sufficient for binding to ELMO, whereas the SH3 domain provides a stabilizing effect in the formation of DOCK180/ELMO complex. (E) $DOCK180^{1-187}$, $DOCK180^{1-422}$, and (F) $DOCK180^{69-187}$ fragments specifically interact with ELMO1 and were visualized by autoradiography according to *Material and Methods*. (G) Hydrophobic residues of a predicted α-helical region between the SH3 and DHR-1 domain of DOCK180 are involved in ELMO1-binding (also see A and Supplementary Figure S4). GST-fusion proteins of the residues 1–200 of $DOCK180^{WT}$, $DOCK180^{L96D/W99E}$, and $DOCK180^{I132D/L133D}$ were used in a pulldown assay with a lysate of Myc-ELMO1-transfected HEK293T cells. Bound proteins were detected by immunoblotting with an anti-Myc antibody.

found that DOCK180$^{\Delta SH3}$ interacts with ELMO1 (Figure 5B) in cotransfection experiments using HEK293T cells. However, deletion of the N-terminal 536 amino acids of DOCK180 (DOCK180$^{\Delta 1-536}$) completely abrogated its ability to interact with ELMO1 (Figure 5B), suggesting the presence of an ELMO1 binding site within the N-terminal region of DOCK180. A series of GST fusion proteins of N-terminal fragments of DOCK180 (1–450, 1–357, 1–250, 1–200, 1–150, 1–100, and 1–69) were generated to delineate this ELMO1-binding site. These studies revealed that the first two hundred amino acids of DOCK180 are required to efficiently pulldown ELMO1 from cell extracts (Figure 5C, colored pink in Figure 5A). Interestingly, in the context of DOCK180 1–200, the W45K mutation in the SH3 domain significantly impairs its ability to precipitate ELMO1 (Figure 5D).

In reverse experiments, we studied whether N-terminal fragments of DOCK180, expressed by in vitro transcription/translation (IVT), were able to associate with GST-ELMO1. Although both DOCK180 1–422 and 1–187 were active in binding ELMO1, a DOCK180 fragment comprising residues 187–603 was incapable of such association (Figure 5E). Next, we tested the ability of GST-ELMO1 to precipitate the IVT DOCK180 fragments 1–69, 1–100, and 69–187. Although no interaction of the SH3 domain-containing fragments of DOCK180 (1–69 and 1–100) to ELMO1 could be detected (Figure 5F), ELMO1 specifically precipitated albeit weakly the DOCK180 69–187 protein (Figure 5F). We conclude that the N-terminal 187 amino acids of DOCK180 harbor the binding site for ELMO proteins, with a primary binding site between residues 69–187. Importantly, we note that in the latter experiments, Rac1 is absent, highlighting that DOCK180/ELMO1 complex formation is Rac1 independent. Interestingly, in these in vitro experiments, more efficient association was observed in the DOCK180 fragment containing the SH3 domain (residues 1–69, Figure 5E), in contrast to some of our coimmunoprecipitation and pulldown experiments. It therefore appears that in the IVT system, the DOCK180/ELMO1 interaction is stabilized by the SH3/PxxP interaction of the two molecules.

Secondary structure prediction of the first 200 amino acids of ELMO-interacting DOCK proteins (DOCK1/DOCK180, 2, 3, 4, and 5) from multiple species uncovered a helical region from residues 80–153 in DOCK180, which overlaps with a highly conserved region in these proteins (Figure 5A, Supplementary Figure S5). We speculated that these predicted helical/coiled-coil regions of DOCK180 might interact directly with the αN-helix of the ELMO1 PH domain in a coiled-coil manner, and hence we designed mutations in two hydrophobic patches within this region in GST-DOCK180 1–200. The mutant proteins were soluble and expressed to similar levels with the wild-type counterpart. Significantly, both resulting proteins, DOCK180 $^{L96D/W99E}$ and DOCK180 $^{I132D/L133D}$, were unable to precipitate ELMO1 from cell extracts (Figure 5G). Hence, within the minimal ELMO1-binding domain of DOCK180, both hydrophobic and SH3-mediated interactions are utilized, and as for ELMO1, mutation of a few hydrophobic amino acids completely disrupts DOCK180/ELMO complex formation.

ELMO1 Does Not Contribute to DOCK180-mediated Rac Activation

Previous findings indicated that complex formation between ELMO1 and DOCK180 promotes the GEF activity of DOCK180 toward Rac by twofold (Brugnera *et al.*, 2002; Lu *et al.*, 2004). In contrast, we demonstrated that DOCK180 alone activates Rac and that the DHR-2 domain of DOCK180 is necessary and sufficient for this activity (Cote and Vuori, 2002; Cote *et al.*, 2005). To clarify this ambiguity, we precipitated the GTP-bound form of Rac1 using the p21-binding domain of PAK1 (PBD assay; Cote and Vuori, 2002). We found that DOCK180 is indispensable for promoting Rac GTP-loading in CHO LR73 cells, and the presence of ELMO1^{WT} did not increase Rac activation (Figure 6A–B). Furthermore, the ELMO1$^{\alpha N/PxxP}$ double mutant defective in DOCK180 binding did not alter Rac GTP-loading in comparison to ELMO1^{WT} (Figure 6A). To ascertain that we performed these Rac activation measurements in the linear range of the assay, we included a condition with saturating amount of DOCK180 (4 μg instead of 1 μg of plasmid). We noted a further increase in Rac activation in comparison to the samples expressing DOCK180 at lower levels, therefore, proving the linearity of the Rac-PBD assay in these conditions (Figure 6A). Similar results were obtained in HEK293T cells (data not shown). To test if DOCK180 can activate Rac in an ELMO-independent manner, a DOCK180 mutant incapable of binding to ELMO1 (DOCK180$^{\Delta 1-536}$) was expressed in HEK293T cells, and Rac activity was measured. We found that much like DOCK180^{WT}, DOCK180$^{\Delta 1-536}$ robustly activated Rac when expressed alone in cells (Figure 6C). As above, we added a control where DOCK180 is expressed to saturation in order to demonstrate that the activities of DOCK180^{WT} and DOCK180 $^{196\ 1-536}$ toward Rac were measured in the linear range of the assay. These results emphasize an intrinsic GEF activity in DOCK180, which is independent of ELMO binding.

Both the PH Domain and PxxP Motifs of ELMO1 Contribute to DOCK180/ELMO1 Signaling

We tested our model of DOCK180/ELMO1 interaction on Rac signaling using functional cell spreading and migration assays in CHO LR73 cells. These cells express endogenous ELMO proteins and DOCK180 (data not shown). We found that exogenous expression of ELMO1^{WT} or ELMO1$^{\alpha N/PxxP}$ had no effect on spreading of LR73 cells on fibronectin when expressed alone (data not shown and Cote *et al.*, 2005). However, when ELMO1^{WT} or ELMO1$^{\alpha N/PxxP}$ were overexpressed in LR73 cells (2 μg instead of 0.3 μg of plasmids), we noted that both proteins could partially interfere with cell spreading, probably by sequestering essential components for Rac signaling (Supplementary Figure S6).

Coexpression of DOCK180/ELMO1/CrkII results in cell elongation when LR73 cells are replated on fibronectin-coated dishes (Cote *et al.*, 2005). We coexpressed ELMO1^{WT} and mutants together with DOCK180 and CrkII and examined the morphology of the transfected cells. In agreement with our biochemical characterization, ELMO1^{PxxP} had no effect on the ability of the ELMO1 protein to promote the elongation of cells when coexpressed with DOCK180 and CrkII (Figure 7, A–C). ELMO1$^{\alpha N}$ prevented signaling from this complex to a small extent, as judged by morphological differences in elongated cells in comparison to the control conditions (Figure 7, A and B). Interestingly, the double mutant ELMO1$^{\alpha N/PxxP}$ markedly prevented cell elongation on fibronectin (Figure 7, A and B).

When the cells were tested for their ability to migrate, similar results were obtained. As reported earlier (Cote *et al.*, 2005), LR73 expressing ELMO1^{WT}/DOCK180/CrkII had an increased capacity to migrate toward fibronectin in a boyden chamber (Figure 7, D and E), and ELMO1^{PxxP} promoted cell migration just as well as its wild-type counterpart (Figure 7, D and E). ELMO1$^{\alpha N}$ led to a slight reduction in the ability of LR73 cells to migrate toward fibronectin (Figure 7, D and E). Mutations in both the αN helix and in the PxxP motif of ELMO1 were required to abrogate the ability of this protein

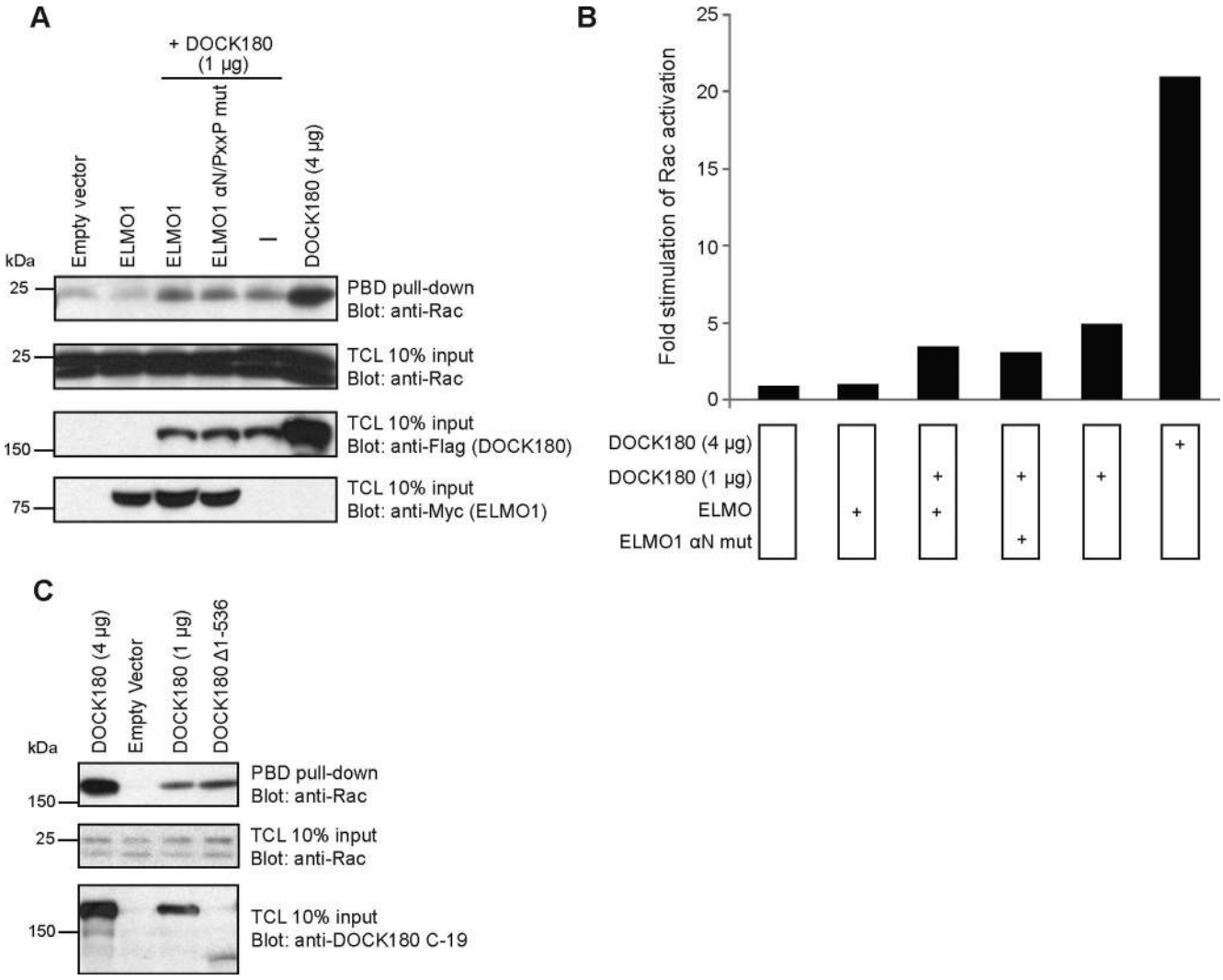

Figure 6. ELMO1 does not contribute toward DOCK180-mediated Rac activation. (A) Rac activation by DOCK180 is independent of ELMO1 in CHO LR73 cells. Cells were transfected with the indicated plasmids and GTP-loaded Rac was pulled down from cell lysates using the p21-binding domain of PAK fused to GST (PBD assay). The amount of Rac in pulldowns and in total cell lysates (TCL) was detected by immunoblotting with an anti-Rac antibody. Expression levels of the various proteins, and equal loading of Rac in all samples, were analyzed by immunoblotting of the TCL using anti-FLAG, anti-Myc, and anti-Rac antibodies. This is a representative experiments from four independent assays. (B) Quantification of Rac activation by the various proteins was performed by densitometry from the experiment in A. (C) A form of DOCK180 lacking the ELMO1-binding region robustly activates Rac. HEK293T cells were transfected with the indicated plasmids and GTP-loaded Rac was pulled down from cell lysates in a PBD assay. The amount of Rac in pulldowns and in total cell lysates (TCL) was detected by immunoblotting with an anti-Rac antibody. Expression levels of the various DOCK180 proteins, and equal loading of Rac in all samples, were analyzed by immunoblotting of the TCL using anti-DOCK180 and anti-Rac antibodies.

to support cell migration (Figure 7, D and E). These results show that ELMO1/DOCK180 complex formation is required for DOCK180 function in cells. Furthermore, the functional data indicate that ectopic expression of ELMO1 mutants display dominant effects without affecting Rac activation. These results strengthen our notion that DHR-2 mediated Rac GEF activity of DOCK180 is ELMO independent.

DISCUSSION

Two Contact Regions between DOCK180 and ELMO1

Analysis of the molecular details of the DOCK180 and ELMO1 interaction has highlighted some inconsistencies (Meller *et al.*, 2005; Cote and Vuori, 2007); however, definitive information is essential for the understanding of Rac activation and signaling mediated by this complex. Here we present data that DOCK180 and ELMO1 interact directly through the N-terminal 187 amino acids of DOCK180 and the C-terminal 195 amino acids of ELMO1 (residues 532–727). The primary interaction between these two regions involves the atypical ELMO1 PH domain (residues 532–707), especially the αN-helix (residues 532–555), and, on DOCK180, a previously uncharacterized region between the SH3 and DHR-1 domains (residues 69–187). Further analysis revealed the existence of an evolutionarily conserved α-helical region (residues 80–153) in DOCK180, which is likely to mediate direct contacts with the atypical hydrophobic αN-helix of the ELMO1 PH domain. A second interaction involves the N-terminal SH3 domain of DOCK180 and the C-terminal PxxP motifs of ELMO1. Our biochemical results

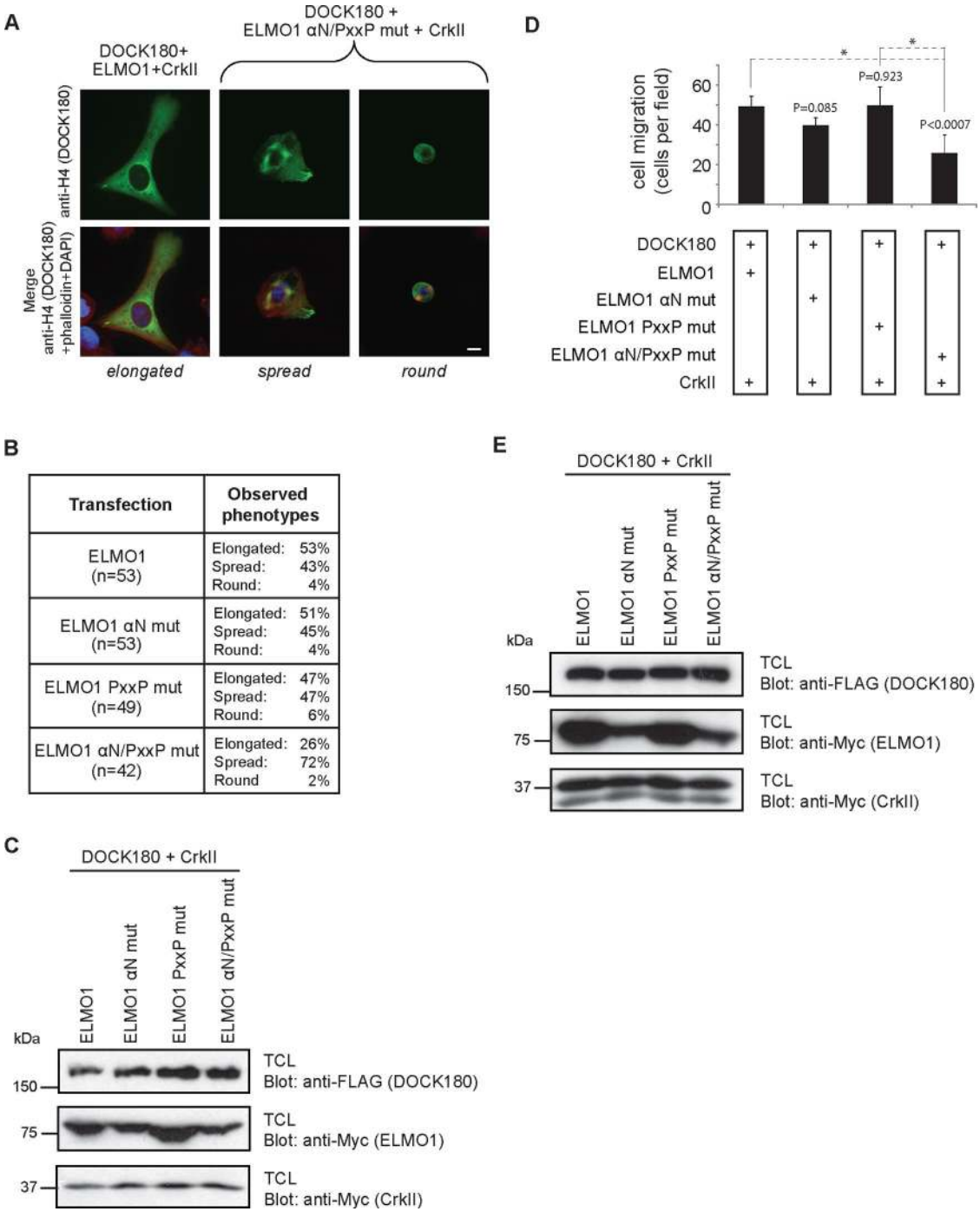

Figure 7. Abrogating DOCK180/ELMO1 interaction in vivo results in defective cell elongation and migration. (A–E) DOCK180/ELMO1 binding is required for proper cell elongation. (A) Serum-starved LR73 cells transfected with the indicated plasmids were detached and plated on fibronectin-coated chambers for 2 h. Cells in the top panels were stained with an antibody against DOCK180 (H-4), whereas bottom panels represent an overlay of the anti-DOCK180, rhodamine-phalloidin, and DAPI stains. Cells were photographed at 100× magnification. Scale bar, 10 μm. (B) Quantification of the effect on cell elongation in response to disruption of the DOCK180/ELMO1 interaction. Several independent fields of the experiments from A were photographed at a magnification of 20×, and cells were scored for three phenotypes: round (attached and minimally spread), spread (clearly spread and flat cells), and elongated (elongated cells with polarity). (C) Expression levels of the transfected proteins for spreading assays were analyzed by immunoblotting cell lysates with anti-FLAG and anti-Myc (ELMO1 and CrkII) antibodies, as indicated. (D) Serum-starved LR73 cells transfected with a GFP vector in addition to the indicated plasmids were detached and placed in the upper compartment of a Boyden chamber. Cells were allowed to migrate for 4 h toward fibronectin and then were fixed and stained with DAPI. GFP/DAPI double-positive cells that migrated to the underside of the membrane were counted from photographs taken at 20× magnification. The migration assay was performed in triplicate, and data are shown as mean ± SD; *$p < 0.002$; one-way ANOVA. (E) Expression levels of the transfected proteins for migration assays were analyzed by immunoblotting cell lysates with anti-FLAG and anti-Myc antibodies, as indicated.

support a mechanism whereby the PH domain of ELMO1 and its flanking regions, especially the αN helix, is the main determinant for binding to DOCK180, whereas the secondary SH3/PxxP interaction is not sufficient to promote complex formation. In cells however, functional analyses revealed that the PxxP motifs in ELMO1 also contribute in promoting efficient cell spreading and cell migration. Our findings in cells correlate with in vivo data in *C. elegans* where both the PH domain and pro-rich region were necessary for the engulfment function of Ced-12 (Zhou *et al.*, 2001). The functional, but not biochemical necessity of the DOCK180 SH3 domain and ELMO1 PxxP motif, might indicate other uncharacterized binding partners for these regions. CrkII and $p130^{Cas}$ are other components that have been implicated to signal to the DOCK180 complex, and these proteins also contain SH3 domains and PxxP motifs. Further structural characterization and identification of additional components of the signaling complexes will be required.

Additional Functions of the PH Domain of ELMO?

The structural analysis of the ELMO1 PH domain enabled a detailed characterization and comparison with other PH domains. We were able to confidently exclude an involvement of the PH domain in PI binding, as the common PI-binding site in ELMO1 is not capable of interacting with such positively charged ligands. Recently, structural analyses of the ESCRT-II GLUE domain (Teo *et al.*, 2006), Tiam1 and ArhGAP9 (Ceccarelli *et al.*, 2007), have revealed a second mode of PH domain–PI interactions through conserved regions outside of the common PI-binding site. In ELMO1 however, this binding site is also different, both at a structural and sequence level.

Instead, we have found strong similarities with FERM domains that contain within their F3 subdomain a PH-like fold and that use the common PI binding site instead as a protein interaction interface (Pearson *et al.*, 2000). Further functional and structural characterization of this putative protein interaction interface is required, but it is tempting to speculate that ELMO may also interact with proteins through this surface.

PH domains appear essential in DOCK GEFs. DOCK1, 2, and 5 and DOCK3 and 4 bind to ELMO and utilize its PH domain, whereas Zizimin1/DOCK9, 10, and 11 contain PH domains themselves in their N-termini (Cote and Vuori, 2007). A structure of the DOCK9 PH domain has recently been deposited in the protein databank (Supplementary Figure S7). This PH domain does not resemble the ELMO1 PH domain, and analysis of the surface potential suggests that it might interact with PIs (Supplementary Material). Indeed, it was recently reported that the DOCK9 PH domain binds to PI ligands and may target DOCK9 to membranes (Meller *et al.*, 2008). Hence, it appears that PH domains of the DOCK GEFs may function in various ways (protein–protein interaction in ELMO/DOCK180 as opposed to membrane interaction in DOCK9), and future research will need to address their roles in more details.

PH Domain of ELMO1: Direct or Indirect Binding to DOCK180 and the Implications for Rac GTP Loading?

A previous study highlighted a fragment of ELMO1, virtually identical to the one characterized here, that was unable to bind DOCK180 directly, but could only interact with a preformed complex between DOCK180 and nucleotide-free Rac (Lu *et al.*, 2004). Mechanistically, these findings were proposed to regulate the catalytic GEF-activity of DOCK180 toward Rac and at least partially explained the bipartite GEF model (Lu *et al.*, 2004), in which DOCK180 and ELMO act somehow together in GDP/GTP exchange. Our detailed mapping of the respective binding sites conflicts with such a *trans* binding mode, as we observe direct interaction independent of Rac. Our structure-based mutagenesis identified key conserved hydrophobic residues in ELMO1 that mediate the direct interaction with DOCK180, and point mutations disrupt this binding. We found that ELMO1 does not affect GTP loading of Rac by DOCK180; however, it is required for signaling to or from the DOCK180/ELMO1 complex. However, as these studies were performed in cells expressing endogenous ELMO1, further studies and knockout models for ELMO family members are required to fully comprehend a contribution of ELMO proteins in DOCK180-mediated Rac GEF activity. The ability of ELMO1 to signal to the actin cytoskeleton likely resides in its N-terminal region where it can bind to ERM proteins and RhoG. These ELMO1-mediated interactions might also play a targeting role (e.g., RhoG resides at the plasma membrane) and in fact point to a role of ELMO1 as an interaction platform for other molecules involved in the pathway. We are now investigating the exciting possibility that ELMO proteins may have a scaffolding function in connecting Rac activators and Rac effectors.

ACKNOWLEDGMENTS

We thank Dr. M. Matsuda (Kyoto University, Kyoto, Japan) for gifts of reagents, Drs. M. Roe and O. Opaleye for data collection, and O. Opaleye also for help in protein purification and crystallization. Coordinates and structure factors have been deposited with the protein data bank, accession number 2vsz. D.K. is supported by a Beit Memorial Fellowship for Medical Research. M.P. and M.L. are supported by Canadian Institutes of Health Research (CIHR) funded scholarships from the Institut de Recherches Cliniques de Montréal Cancer Training Program. This work was supported by a CIHR operating grant (J.-F.C.) and Cancer Research UK (D.B.). J.-F.C. holds a CIHR New Investigator Award.

REFERENCES

Bailey, S. (1994). The Ccp4 suite—program for protein crystallography. Acta Crystallogr. D Biol. Crystallogr. *750*, 760–763.

Bianco, A., Poukkula, M., Cliffe, A., Mathieu, J., Luque, C. M., Fulga, T. A., and Rorth, P. (2007). Two distinct modes of guidance signalling during collective migration of border cells. Nature *448*, 362–365.

Bowzard, J. B., Cheng, D., Peng, J., and Kahn, R. A. (2007). ELMOD2 is an Arl2 GTPase-activating protein that also acts on Arfs. J. Biol. Chem. *282*, 17568–17580.

Bricogne, G., Vonrhein, C., Flensburg, C., Schiltz, M., and Paciorek, W. (2003). Generation, representation and flow of phase information in structure determination: recent developments in and around SHARP 2.0. Acta Crystallogr. *59*, 2023–2030.

Brugnera, E., Haney, L., Grimsley, C., Lu, M., Walk, S. F., Tosello-Trampont, A. C., Macara, I. G., Madhani, H., Fink, G. R., and Ravichandran, K. S. (2002). Unconventional Rac-GEF activity is mediated through the Dock180-ELMO complex. Nat. Cell Biol. *4*, 574–582.

Brunger, A. T. *et al.* (1998). Crystallography & NMR system: a new software suite for macromolecular structure determination. Acta Crystallogr. *54*, 905–921.

Ceccarelli, D. F., Blasutig, I. M., Goudreault, M., Li, Z., Ruston, J., Pawson, T., and Sicheri, F. (2007). Non-canonical interaction of phosphoinositides with pleckstrin homology domains of Tiam1 and ArhGAP9. J. Biol. Chem. *282*, 13864–13874.

Chung, S., Gumienny, T. L., Hengartner, M. O., and Driscoll, M. (2000). A common set of engulfment genes mediates removal of both apoptotic and necrotic cell corpses in. *C. elegans.* Nat. Cell Biol. *2*, 931–937.

Cote, J. F., Motoyama, A. B., Bush, J. A., and Vuori, K. (2005). A novel and evolutionarily conserved PtdIns(3,4,5)P3-binding domain is necessary for DOCK180 signalling. Nat. Cell Biol. *7*, 797–807.

Cote, J. F., and Vuori, K. (2002). Identification of an evolutionarily conserved superfamily of DOCK180-related proteins with guanine nucleotide exchange activity. J. Cell Sci. *115*, 4901–4913.

Cote, J. F., and Vuori, K. (2007). GEF what? Dock180 and related proteins help Rac to polarize cells in new ways. Trends Cell Biol. *17*, 383–393.

Emsley, P., and Cowtan, K. (2004). Coot: model-building tools for molecular graphics. Acta Crystallogr. *60*, 2126–2132.

Ferguson, K. M., Kavran, J. M., Sankaran, V. G., Fournier, E., Isakoff, S. J., Skolnik, E. Y., and Lemmon, M. A. (2000). Structural basis for discrimination of 3-phosphoinositides by pleckstrin homology domains. Mol. Cell *6*, 373–384.

Ferguson, K. M., Lemmon, M. A., Schlessinger, J., and Sigler, P. B. (1995). Structure of the high affinity complex of inositol trisphosphate with a phospholipase C pleckstrin homology domain. Cell *83*, 1037–1046.

Grimsley, C. M., Kinchen, J. M., Tosello-Trampont, A. C., Brugnera, E., Haney, L. B., Lu, M., Chen, Q., Klingele, D., Hengartner, M. O., and Ravichandran, K. S. (2004). Dock180 and ELMO1 proteins cooperate to promote evolutionarily conserved Rac-dependent cell migration. J. Biol. Chem. *279*, 6087–6097.

Grimsley, C. M., Lu, M., Haney, L. B., Kinchen, J. M., and Ravichandran, K. S. (2006). Characterization of a novel interaction between ELMO1 and ERM proteins. J. Biol. Chem. *281*, 5928–5937.

Gumienny, T. L. *et al.* (2001). CED-12/ELMO, a novel member of the CrkII/Dock180/Rac pathway, is required for phagocytosis and cell migration. Cell *107*, 27–41.

Handa, Y., Suzuki, M., Ohya, K., Iwai, H., Ishijima, N., Koleske, A. J., Fukui, Y., and Sasakawa, C. (2007). *Shigella* IpgB1 promotes bacterial entry through the ELMO-Dock180 machinery. Nat. Cell Biol. *9*, 121–128.

Hiramoto, K., Negishi, M., and Katoh, H. (2006). Dock4 is regulated by RhoG and promotes Rac-dependent cell migration. Exp. Cell Res. *312*, 4205–4216.

Holm, L., and Sander, C. (1993). Protein structure comparison by alignment of distance matrices. J. Mol. Biol. *233*, 123–138.

Hulo, N., Bairoch, A., Bulliard, V., Cerutti, L., Cuche, B. A., de Castro, E., Lachaize, C., Langendijk-Genevaux, P. S., and Sigrist, C. J. (2008). The 20 years of PROSITE. Nucleic Acids Res. *36*, D245–D249.

Katoh, H., and Negishi, M. (2003). RhoG activates Rac1 by direct interaction with the Dock180-binding protein Elmo. Nature *424*, 461–464.

Kiyokawa, E., Hashimoto, Y., Kobayashi, S., Sugimura, H., Kurata, T., and Matsuda, M. (1998). Activation of Rac1 by a Crk SH3-binding protein, DOCK180. Genes Dev. *12*, 3331–3336.

Komander, D., Fairservice, A., Deak, M., Kular, G. S., Prescott, A. R., Peter Downes, C., Safrany, S. T., Alessi, D. R., and van Aalten, D. M. (2004). Structural insights into the regulation of PDK1 by phosphoinositides and inositol phosphates. EMBO J. *23*, 3918–3928.

Lemmon, M. A., and Ferguson, K. M. (2000). Signal-dependent membrane targeting by pleckstrin homology (PH) domains. Biochem. J. *350*(Pt 1), 1–18.

Li, X., Gao, X., Liu, G., Xiong, W., Wu, J., and Rao, Y. (2008). Netrin signal transduction and the guanine nucleotide exchange factor DOCK180 in attractive signaling. Nat. Neurosci. *11*, 28–35.

Lu, M. *et al.* (2004). PH domain of ELMO functions in trans to regulate Rac activation via Dock180. Nat. Struct. Mol. Biol. *11*, 756–762.

Lu, M., Kinchen, J. M., Rossman, K. L., Grimsley, C., Hall, M., Sondek, J., Hengartner, M. O., Yajnik, V., and Ravichandran, K. S. (2005). A Steric-inhibition model for regulation of nucleotide exchange via the Dock180 family of GEFs. Curr. Biol. *15*, 371–377.

Meller, N., Merlot, S., and Guda, C. (2005). CZH proteins: a new family of Rho-GEFs. J. Cell Sci. *118*, 4937–4946.

Meller, N., Westbrook, M. J., Shannon, J. D., Guda, C., and Schwartz, M. A. (2008). Function of the N-terminus of zizimin 1, autoinhibition and membrane targeting. Biochem. J. *409*, 525–533.

Morris, R. J., Perrakis, A., and Lamzin, V. S. (2003). ARP/wARP and automatic interpretation of protein electron density maps. Methods Enzymol. *374*, 229–244.

Pape, T., and Schneider, T. (2004). Hkl2map: a graphical user interface for macromolecular phasing with shelx programs. J. Appl. Crystallogr. *37*, 843–844.

Pearson, M. A., Reczek, D., Bretscher, A., and Karplus, P. A. (2000). Structure of the ERM protein moesin reveals the FERM domain fold masked by an extended actin binding tail domain. Cell *101*, 259–270.

Rushton, E., Drysdale, R., Abmayr, S. M., Michelson, A. M., and Bate, M. (1995). Mutations in a novel gene, myoblast city, provide evidence in support of the founder cell hypothesis for *Drosophila* muscle development. Development *121*, 1979–1988.

Tanaka, M., Gupta, R., and Mayer, B. J. (1995). Differential inhibition of signaling pathways by dominant-negative SH2/SH3 adapter proteins. Mol. Cell. Biol. *15*, 6829–6837.

Teo, H., Gill, D. J., Sun, J., Perisic, O., Veprintsev, D. B., Vallis, Y., Emr, S. D., and Williams, R. L. (2006). ESCRT-I core and ESCRT-II GLUE domain structures reveal role for GLUE in linking to ESCRT-I and membranes. Cell *125*, 99–111.

Vagin, A. A., Steiner, R. A., Lebedev, A. A., Potterton, L., McNicholas, S., Long, F., and Murshudov, G. N. (2004). REFMAC5 dictionary: organization of prior chemical knowledge and guidelines for its use. Acta Crystallogr. *60*, 2184–2195.

Wu, Y. C., Cheng, T. W., Lee, M. C., and Weng, N. Y. (2002). Distinct rac activation pathways control *Caenorhabditis elegans* cell migration and axon outgrowth. Dev. Biol. *250*, 145–155.

Wu, Y. C., and Horvitz, H. R. (1998). *C. elegans* phagocytosis and cell-migration protein CED-5 is similar to human DOCK180. Nature *392*, 501–504.

Wu, Y. C., Tsai, M. C., Cheng, L. C., Chou, C. J., and Weng, N. Y. (2001). *C. elegans* CED-12 acts in the conserved crkII/DOCK180/Rac pathway to control cell migration and cell corpse engulfment. Dev. Cell *1*, 491–502.

Zhou, Z., Caron, E., Hartwieg, E., Hall, A., and Horvitz, H. R. (2001). The *C. elegans* PH domain protein CED-12 regulates cytoskeletal reorganization via a Rho/Rac GTPase signaling pathway. Dev. Cell *1*, 477–489.